Physica Medica 42 (2017) 263–270

Contents lists available at ScienceDirect

Physica Medica

journal homepage: http://www.physicamedica.com

Original paper

Comparative study of the calculated risk of radiation-induced cancer after photon- and proton-beam based radiosurgery of liver metastases

Gracinda Mondlane [a,b,*], Michael Gubanski [c], Pehr A. Lind [c,d], Ana Ureba [a], Albert Siegbahn [a]

[a] Department of Physics – Medical Radiation Physics, Stockholm University, Stockholm, Sweden
[b] Department of Physics, Universidade Eduardo Mondlane, Maputo, Mozambique
[c] Department of Oncology and Pathology, Karolinska University Hospital, Stockholm, Sweden
[d] Department of Oncology, Södersjukhuset, Stockholm, Sweden

ARTICLE INFO

Article history:
Received 14 December 2016
Received in Revised form 21 February 2017
Accepted 21 March 2017
Available online 31 March 2017

Keywords:
Liver metastases
Secondary cancers
SBRT
IMPT

ABSTRACT

Introduction: The potential of proton therapy to improve the sparing of the healthy tissue has been demonstrated in several studies. However, even small doses delivered to the organs at risk (OAR) may induce long-term detriments after radiotherapy. In this study, we investigated the possibility to reduce the risk of radiation-induced secondary cancers with intensity modulated proton therapy (IMPT), when used for radiosurgery of liver metastases.

Material and methods: Ten patients, previously treated for liver metastases with photon-beam based stereotactic body radiation therapy (SBRT) were retrospectively planned for radiosurgery with IMPT. A treatment plan comparison was then performed in terms of calculated risk of radiation-induced secondary cancer. The risks were estimated using two distinct models (Dasu et al., 2005; Schneider et al., 2005, 2009). The plans were compared pairwise with a two-sided Wilcoxon signed-rank test with a significance level of 0.05.

Results: Reduced risks for induction of fatal and other types of cancers were estimated for the IMPT plans ($p < 0.05$) with the Dasu et al. model. Using the Schneider et al. model, lower risks for carcinoma-induction with IMPT were estimated for the skin, lungs, healthy part of the liver, esophagus and the remaining part of the body ($p < 0.05$). The risk of observing sarcomas in the bone was also reduced with IMPT ($p < 0.05$).

Conclusion: The findings of this study indicate that the risks of radiation-induced secondary cancers after radiosurgery of liver metastases may be reduced, if IMPT is used instead of photon-beam based SBRT.

1. Introduction

Proton-beam therapy (PBT) is an emerging form of radiotherapy (RT) used for cancer treatment. A reduction in the number of observed long-term side effects can be expected after proton beam radiotherapy [1–4], due to the decreased integral doses delivered to the risk organs [5]. The reduced risks of inducing secondary malignancies have also been stated as a rationale for the implementation of proton beams in the clinic. This advantage has been emphasized mainly for the radiotherapy of paediatric patients [6–8]. However, in the last decades, advances in cancer diagnostics as well as in systemic treatment options, in combination with a variety of local treatment modalities, have led to increasing survival rates and life expectancy, even for patients receiving RT late in life. This makes the incidence of cancer induction after RT pertinent also for adult RT patients [9,10].

The frequency of radiation-induced cancer in human tissues, after total body exposures with low doses of ionizing radiation, has been determined in different epidemiological studies [11–14]. However, these studies involve doses (<100 mSv) which are lower than those used in RT, for which the dose-response can be described with the linear non-threshold (LNT) model. It is well-known that the LNT model overestimates the risks for higher doses, as it does not account for cell kill which decreases the cancer risk [15,16]. Different dose-response models, valid for all doses, have been proposed [15–18]. These models predict a linear increase of risk with dose in the low dose region. At higher doses, some models predict an exponential decrease of the risk with increasing doses. Other models assume risk saturation at high doses. Due to the fact that the estimated cancer-risk depends on

* Corresponding author at: Department of Medical Radiation Physics, Stockholm University, Box 260, 171 76 Stockholm, Sweden.
E-mail address: gracinda.mondlane@fysik.su.se (G. Mondlane).

http://dx.doi.org/10.1016/j.ejmp.2017.03.019
1120-1797/

the dose heterogeneity across the irradiated organ and on the type of tissue irradiated, these factors should be included in the risk estimation.

A photon-based radiosurgery technique called stereotactic body radiation therapy (SBRT) has been developed, with which high lethal doses can be delivered to targets in the liver with low toxicity. It has been suggested that hypofractionated RT could reduce the frequency of radiation-induced secondary cancers, compared to conventionally fractionated RT [19]. The age at the time of treatment is in general high for patients receiving radiosurgery of liver metastases [20]. However, a large fraction of the patients treated have been found to be long-term survivors [20–22], which has made the late side effects more relevant.

Radiosurgery implemented with proton beams have been proposed for the treatment of liver metastases. Dosimetric studies, comparing photon- and proton-beam therapy for the treatment of oligo-metastases in the liver [22–24] have reported that the doses given to normal tissues can be reduced with PBT. This is in particular the case for the doses given to the normal part of the liver, the main OAR in radiation therapy of malignancies in the liver.

In a recent dosimetric study of radiosurgery of liver metastases, involving patients included in the present study [24], the OARs were found to be better spared from irradiation with low and intermediate doses with the intensity modulated proton therapy (IMPT) technique. However, stochastic effects which lead to cancer induction may occur at all dose levels [25]. Therefore, to be able to compare the risk of radiation-induced cancer, produced with different RT modalities, the risks need to be quantified with the suggested radiation-risk models. The aim of this study was to use radiobiological models to investigate the potential of IMPT to reduce the risk of inducing secondary malignancies after radiosurgery of liver metastases.

2. Material and methods

2.1. Patient selection and treatment planning

Ten patients diagnosed with liver metastases from primary colorectal cancer were included in this study (median age of 77 years and range 66 – 89 years). These patients were treated with photon-based SBRT at the Department of Oncology and Pathology at Karolinska University Hospital and were selected based on the tumour size and location within the liver (Table 1), as representative cases for this patient group. A summary of the treatment characteristics is also shown in Table 1.

The planning computed tomography (CT) image sets consisted of 3.0 mm thick slices. The dose calculations, carried out as part of the treatment planning, were based on patient-composition data from regular free-breathing CT studies. The ITV concept was used to take the target motion into consideration in the planning. The CTV to ITV expansion margins were determined using 4D-CT studies. The ITV to PTV margins were set to 5 mm in the transversal direction and 10 mm in the cranio-caudal direction. Two distinct SBRT treatment techniques were used to create the photon plans, the static-field three-dimensional conformal radiotherapy (3D-CRT) technique (7 patients) and the volumetric modulated arc therapy (VMAT) technique (3 patients). VMAT was used to treat the patients with large target volumes (patients 3 and 6) or when critical structures were located close to the target (patient 8), (Table 1). These photon plans, used for the actual treatments, were used as reference plans in the comparison with the prepared IMPT plans. The stereotactic frame, used for patient immobilization, was assigned the Hounsfield unit of air in the planning CT study used for the IMPT planning in order to avoid uncertainties specific for the proton dose calculation.

A two-field IMPT technique was used to retrospectively plan all the patients. The planning objective was set to achieve a similar PTV dose coverage as with the original photon plans. In these plans, the periphery of the PTV received 100% of the prescribed dose and in the center of the target volume, where presumably the more radio-resistant cells were located, doses in the range from 145% to 160% of the prescribed dose were allowed. The healthy part of the liver was identified as the most critical OAR. Other OARs considered were the skin, kidneys, lungs, esophagus, bone and spinal cord. Direct irradiations through the spinal cord and the right kidney were avoided in the IMPT planning. The assessment of risk for treatment-induced secondary malignancies was also performed for the remaining tissues (the part of the body encompassed by the CT study that was not delineated as OARs), referred to as "other-solid".

The treatment planning was performed with the Eclipse treatment planning system (TPS) (Varian Medical Systems, Palo Alto, California, version 11.0.42). Photon beams of energy 6 MV, produced by a Varian (Varian Medical Systems, Palo Alto, California) linear accelerator, were used for the photon-beam therapy planning. The proton-beam data was taken from a facility with an IBA cyclotron (Ion Beam Applications S.A., Louvain-La-Neuve, Belgium) with initial proton energies varying between 60 and 230 MeV. A generic relative biologic effectiveness (RBE) value of 1.1 was assumed for the proton beams.

2.2. Estimation of the risk for radiation-induced secondary cancer

The cancer-risk calculations were performed using data extracted from the dose-volume histograms (DVHs) generated in the treatment planning process. The estimation of the risk for radiation-induced secondary malignancies following radiotherapy was performed using two distinct calculation models. One of these models, the competition model (competition between mutation induction and cell kill), was first proposed by UNSCEAR [17] and later adapted by Dasu et al. [15] to account for both treatment dose fractionation and dose heterogeneity within the OARs. The other model, proposed by Schneider and co-authors [16,18], is based

Table 1
Patient setup and description of the photon-beam treatment.

Patient #	Modality (photon SBRT)	Fractionation	Abdominal pressure	PTV (cm^3)	Target location
1	Static fields	15 Gy x 3	Yes	59.6	Central-peripheral
2	Static fields	17 Gy x 3	Yes	73.1	Superior
3	VMAT	8 Gy x 7	No	332.3	Posterior/whole liver extent axially
4	Static fields	8 Gy x 5	Yes	302.6	Central/whole liver extent axially
5	Static fields	7 Gy x 8	No	66.4	Central-periphery
6	VMAT	7 Gy x 8	No	294.1	Central-superior
7	Static fields	15 Gy x 3	No	18.6	Central-periphery
8	VMAT	7 Gy x 8	Yes	78.6	Superior
9	Static fields	17 Gy x 3	No	30.2	Central
10	Static fields	15 Gy x 3	No	72.3	Central

on a metric called the *organ equivalent dose* (OED) which can be determined with different dose-response relationships. In this model, besides mutation induction and cell kill, repopulation/repair can also be considered to estimate the risks for inducing carcinomas and sarcomas.

From here on, the competition model will be referred to as the Dasu-model and the model based on the OED will be referred to as the Schneider-model. A pairwise two-sided Wilcoxon signed-rank test, with a significance level of 0.05, was then performed of the results obtained with the Dasu- and with the Schneider-model.

2.3. The Dasu-model

The competition model is a linear-quadratic (LQ)-based model (Eq. (1)).

$$Total\,risk_{organ} = \frac{1}{\sum_i v_i}\sum_i v_i \times \left\{ \left(\alpha_1 D_i + \frac{\beta_1 D_i^2}{n}\right) \times exp\left[-\left(\alpha_2 D_i + \frac{\beta_2 D_i^2}{n}\right)\right]\right\} \tag{1}$$

where v_i is the volume of tissue receiving a dose D_i and n is the number of fractions used. The parameters α_1 and β_1 describe the induction of carcinogenic mutations and α_2 and β_2 describe the cell survival in the irradiated organs. The parameters α_1 and α_2 are shown in Table 2. The parameter α_1 was calculated using the sex-averaged nominal risks coefficients for fatal- and total-risk of induction of cancers given by the ICRP Publication 103 [25] (see Table 2). For proton beams, a radiation weighting factor of 2 (w_R as defined by ICRP 103) [25] was used in the conversion of the risk coefficients, to account for the difference in biological effectiveness compared to photon beams. The parameter β_1 was calculated under the assumption that the probability of induction of mutations and the probability of cell kill are described by the same α/β parameter. A value of the α/β parameter of 3 Gy was assumed for all the OARs (skin, lungs, healthy part of the liver, esophagus, bone and other-solid). The risk of observing cancer after radiotherapy in any part of the body was then calculated as the sum of the risks obtained for the individual organs and tissues encompassed by the planning CT image studies.

2.4. The Schneider-model

The risks for inducing carcinomas and sarcomas were also estimated using the model proposed by Schneider and co-authors, based on determination of the so-called OED [16] (Eq. (2)).

$$OED = \frac{1}{\sum_i v_i}\sum_i v_i \times RED(D_i) \tag{2}$$

where v_i and D_i are defined as for Eq. (1) and $RED(D_i)$ is the selected dose-response relationship.

Table 2
Risk coefficients (α_1, second and third column) and the linear quadratic model parameter (last column) used for risk assessment for the different organs at risk. The risk coefficients were taken from ICRP 103 [25]. The linear LQ-model parameters were adapted from Schneider et al. [16], except the value for the spinal cord, which was taken from Kehwar [42].

Organ	α_1 (Gy^{-1}) (fatal risk)	α_1 (Gy^{-1}) (total risk)	α_2 (Gy^{-1})
Skin	0.0002	0.1000	0.047
Lung	0.0101	0.0144	0.129
Normal liver	0.0028	0.0030	0.487
Esophagus	0.0014	0.0015	0.274
Bone	0.0003	0.0007	0.033
Spinal cord	–	–	0.044
Other solid	0.0028	0.0144	0.080

With this model, the risk of observing treatment-induced carcinomas was estimated with three distinct dose-response relationships: the linear, linear-exponential and plateau relationships. The linear relationship predicts a linear increase of the risk with increasing doses. With this model, the mean dose given to the whole organ can be used to calculate the risk. The linear-exponential and the plateau models were derived from a mechanistic equation which, besides the induction of mutations and cell kill also takes the repopulation/repair and treatment fractionation into account (Eq. (3)) [18].

$$RED(D_i) = \frac{e^{-\alpha' D_i}}{\alpha' R}\left(1 - 2R + R^2 e^{\alpha' D_i} - (1-R)^2 e^{-\frac{\alpha' R}{1-R} D_i}\right) \tag{3}$$

where, R describes the repopulation/repair of the irradiated cells between two dose fractions. It has a value of 0 if no repair occurs and 1 if full repair is observed. The parameter α' is defined using the LQ model and it is proportional to the number of cells which are reduced by cell killing:

$$\alpha' = \alpha + \beta \frac{D_i}{n} \tag{4}$$

where n is the number of fractions used. The values of α in Eq. (4) are presented in the last column of Table 2 as α_2. The linear-exponential dose-response relationship is obtained from Eq. (3) by completely neglecting the repopulation/repair effect, i.e., in the limit of $R \to 0$. The plateau dose-response relationship is obtained from Eq. (3) by considering that complete repopulation/repair takes place, i.e., in the limit of $R \to 1$. The three equations describing the dose-response relationships for the linear, linear-exponential and the plateau models, respectively, are shown in Eq. (5).

$$RED(D_i) = \begin{cases} D_i \\ D_i e^{-\alpha' D_i} \\ \frac{1 - e^{-\alpha' D_i}}{\alpha'} \end{cases} \tag{5}$$

For the induction of sarcomas, a mechanistic dose-response relationship which takes cell kill and dose fractionation into account was used (Eq. (6)). A minimal repair/repopulation was considered by using a value for the parameter R of 0.1. This level of repair/repopulation was chosen for this work since the patients in our study received hypofractionated treatments.

$$RED(D_i) = \frac{e^{-\alpha' D_i}}{\alpha' R}\left(1 - 2R + R^2 e^{\alpha' D_i} - (1-R)^2 e^{-\frac{\alpha' R}{1-R} D_i} - \alpha' R D_i\right) \tag{6}$$

The relative risks for inducing carcinomas and sarcomas were calculated as the ratio of the OEDs obtained for specific OARs in the two plans compared (the IMPT plan relative to the SBRT plan). The risk of observing carcinoma was calculated for the skin, the lungs, the normal liver, the esophagus, the spinal cord and "other-solid", and the risk for observing sarcomas was estimated for bone. As for the Dasu-model, an α/β value of 3 Gy was assumed for all the OARs in the calculation of risk for radiation-induced malignancies with the Schneider-model.

3. Results

Regarding the target dose-coverage, the treatment planning objectives were fulfilled in all IMPT plans. With these plans, the doses given to most of the OARs were reduced [24]. Calculated dose distributions in the axial plane for two patients planned for SBRT, implemented with fixed-field photon beams (3D-CRT) or with VMAT (representing one case with a small PTV (patient 3) and one case with a large PTV (patient 7)), are shown in Fig. 1. The dose distributions calculated for the corresponding IMPT plans for these two patients, are also presented.

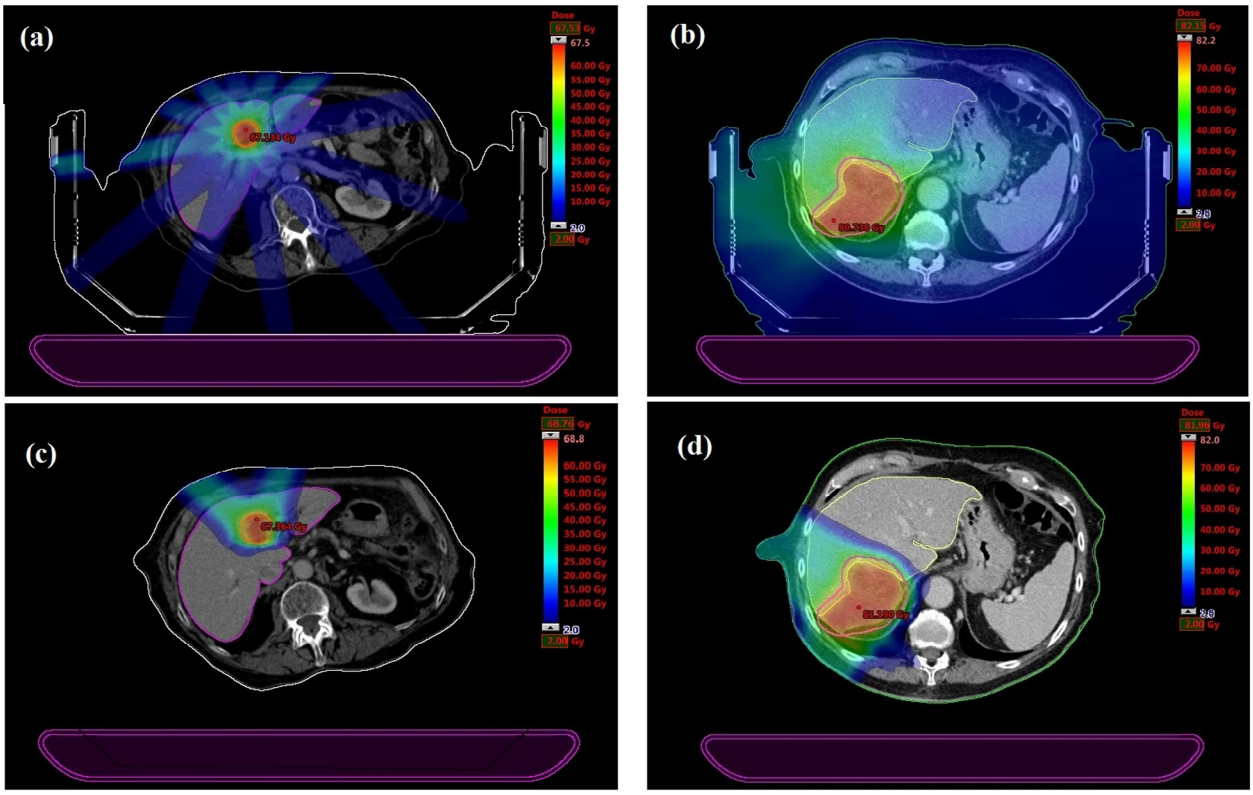

Fig. 1. Dose distributions in two patients (left: patient 7; right: patient 3) planned with (a) fixed-field (3D-CRT) photon SBRT and (b) SBRT implemented with VMAT. The corresponding two-field IMPT plans for these patients are presented in (c) and (d), respectively.

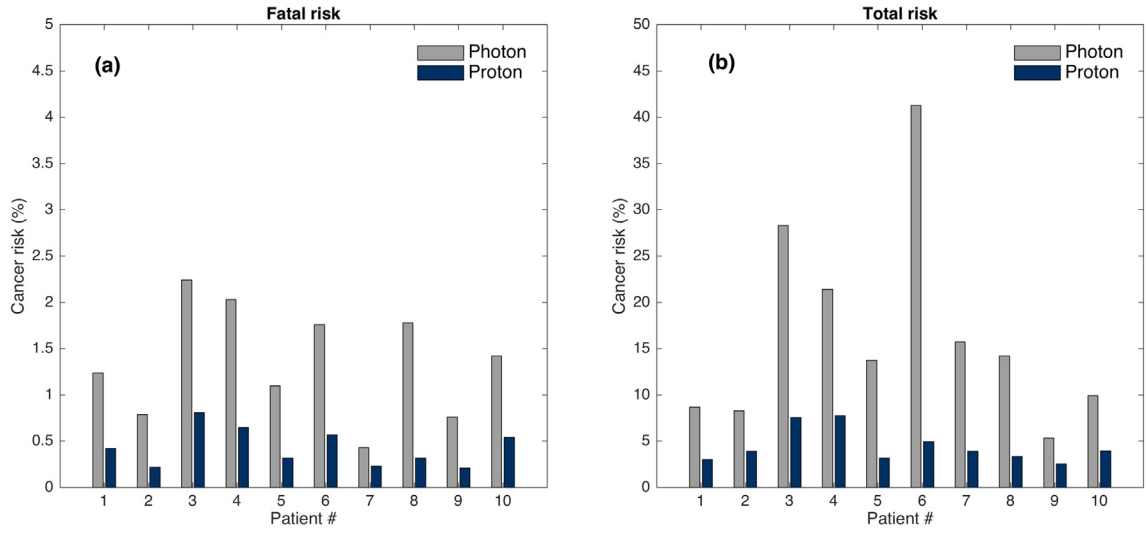

Fig. 2. Calculated whole-body risks of fatal cancer induction (a) and total risks of cancer induction (b) for the SBRT-plans (photon-beam based) and IMPT-plans (proton-beam based), estimated using the Dasu-model.

The risk for inducing fatal cancer and the total risk for observing any type of radiation-induced secondary cancer, estimated using the Dasu-model, are presented in Fig. 2 for each patient. The risk of fatal cancer decreased from a median value of 1% (0%–2%) in the SBRT plans to 0% (0%–1%) in the IMPT plans ($p < 0.05$) and the total risk for observing secondary neoplasms of any type after radiotherapy decreased from a median value of 14% (5%–41%) in the SBRT plans to 4% (3%–8%), in the IMPT plans ($p < 0.05$).

When using the Schneider-model for estimating the risk of inducing carcinomas and sarcomas, the ratios of the OED values obtained from the IMPT and SBRT plans were determined, which resulted in the relative risks presented in Table 3. The ratios of the risks for carcinoma induction were below unity for the different OARs, showing that these risks were consistently lower for the IMPT plans ($p < 0.05$), with only one exception. For patient 3, a relative risk of 1.7 was obtained for the healthy part of the liver with the linear-exponential dose-response relationship ($p < 0.05$). The risk of inducing sarcomas in the bone was also lower with the IMPT plans (Table 3). A summary of the calculated relative risks of carcinoma induction in the skin, lungs, normal liver, esophagus,

Table 3
Median values (range) of the relative risks for observing carcinomas (skin, lung, normal liver, esophagus, spinal cord and other solid) and sarcomas (bone), assessed using the Schneider-model.

	Organ	IMPT/SBRT relative risk of cancer		
		Linear	Linear-Exponential	Plateau
Carcinoma	Skin	0.3 (0.2–0.5)	0.2 (0.1–0.3)	0.2 (0.1–0.3)
	Lung	0.2 (0.1–0.7)	0.2 (0.1–0.5)	0.2 (0.1–0.5)
	Normal liver	0.6 (0.3–0.9)	0.4 (0.2–1.7)	0.4 (0.2–0.6)
	Esophagus	0.1 (0.0–0.4)	0.3 (0.1–0.7)	0.2 (0.0–0.5)
	Spinal cord	0.0 (0.0–0.2)	0.1 (0.0–0.2)	0.0 (0.0–0.2)
	Other solid	0.3 (0.2–0.5)	0.2 (0.1–0.2)	0.2 (0.1–0.3)
Sarcoma	Bone		0.5 (0.2–0.7)*	

$p < 0.05$ in the comparisons of the risks determined pairwise for all the OARs with the SBRT and IMPT plans.
* The result for sarcoma induction was calculated with a specific dose-response relationship for sarcomas.

spinal cord and other-solid is presented in Fig. 3 for the three distinct dose-response relationships. The calculated relative risks for inducing sarcoma (for bone) are also shown.

4. Discussion

In the present study, we performed a pairwise comparison of the estimated individual risks of radiation-induced secondary malignancies for liver metastases patients treated with photon-beam based SBRT and then later retrospectively planned for IMPT. We found that the calculated risks of radiation-induced secondary cancers were lower for IMPT-based radiosurgery, using both the Dasu- and Schneider-model for cancer-risk estimation.

With the Dasu-model, the risk of observing skin cancer (melanoma) gave the largest individual contribution to the total risk of cancer (between 72% and 94% of the total risk calculated for SBRT and between 75% and 88% of the total risk calculated for IMPT). On the other hand, in the risk assessment carried out with the Schneider-model, the highest values of the OED were registered for the healthy part of the liver for both the SBRT- and IMPT-plans. Relative risks closer to unity were calculated for this organ, indicating that the risk reduction achievable with IMPT was not large. Furthermore, an analysis of the results obtained with the Dasu-model showed that the highest cancer-induction risks were obtained for the patients with the largest PTV volumes, *i.e.*, patients 3, 4 and 6 (Table 1). This is due to the fact that a larger target volume implies larger volumes of the healthy tissue irradiated.

Higher relative cancer-risks (Schneider-model) were calculated with the linear dose-risk relationship, except for the esophagus and spinal cord. For the former organ, the linear model predicted the lowest relative risk, while for the latter organ, comparable risk values were obtained with the three different dose-response relationships. The highest relative risk was determined for the normal liver tissue, with the linear dose-response relationship. With this model, the risk is proportional to the organ mean dose, which was highest for the liver.

The major contribution to the cancer-risks comes from the primary radiation [26]. However, to provide a complete description of the cancer-induction risks for a specific RT technique, the dose deposition produced by the different kinds of secondary radiation present during the treatment, which is considered to be of importance for cancer induction, *e.g.* neutrons, should also be taken into account [27]. We did not calculate the specific risk produced by secondary neutrons in this work. The standard TPS used clinically (also used for this work) does not perform neutron transport. The doses deposited by other types of scatter radiation, e.g. out-of-field stray photons in photon RT, are also normally not calculated accurately with standard TPSs. To accurately assess the doses deposited by scattered out-of-field radiation, direct phantom measurements and Monte Carlo calculations have been performed [3,26,28]. In one of these studies [28], a 40% reduction of the cancer-risk was calculated for passively-scattered proton beam treatments of hepatocellular carcinoma, compared to 6-MV IMRT treatments. In another study [26], involving 30 prostate-cancer patients, a reduction of the risk of secondary cancer of approximately 50% was obtained for PBS, compared to the photon beam treatment. The irradiation setup used for different treatments must be considered since it determines the tissue volume irradiated and which dose that is given to the surrounding healthy tissue. Despite the fact that these two studies report results for two different tumour sites, the reduction in cancer risk with PBS was large and partly connected to the reduced secondary-neutron doses in PBS, compared to passive-scattering proton beams.

It has been shown that the neutron dose-equivalent decreases rapidly with increasing distance from the beam [3,29]. Schneider et al. [29] reported that, for a medium-sized target volume, the maximum neutron dose-equivalent in the beam, found in the Bragg peak region (177-MeV PBS), is approximately 1% of the treatment dose and therefore practically irrelevant for cancer induction in those regions. The relative importance of the neutron dose increases with distance from the beam due to the long range of neutrons in tissue. For the healthy tissues located outside of the beam, typical equivalent neutron dose of a few mSv per treatment Gy have been determined for medium-size target volumes. Using phantom measurements, Yoon et al. [3] compared the out-of-field doses produced in head-and-neck and prostate cancer treatments after IMRT (scattered photons) and passive-scattered proton therapy (secondary neutrons). The cancer-risk arising from this out-of-field radiation was also estimated using the OED approach. For the prostate cancer patients, the secondary equivalent doses produced in the IMRT treatments were found to be one order of magnitude higher than those produced in the proton-beam treatments. The calculated risk of secondary cancer produced by the out-of-field doses were 5 times higher for the IMRT treatments for these patients, compared to the passive-scattered proton – beam treatments. For the head-and-neck patients, no significant differences in the equivalent doses were found. The lower neutron doses produced in PBS will most likely result in further decreases of the cancer-risk for the out-of-field organs.

RT delivered with conventional fractionation schemes has historically only had a limited role in the treatment of non-resectable primary or metastatic malignancies in the liver due to the risk of treatment induced toxicity [30]. The use of ablative doses to small target volumes, as in SBRT, has led to reduced levels of toxicity while providing effective local control, in the management of liver malignancies [31]. However, the delivery of high radiosurgery doses to targets in the liver requires high accuracy in patient positioning and motion management, especially when using PBS. Motion management for the patients included in this study was performed by using the ITV concept and in some cases abdominal compression was applied. The use of large margins

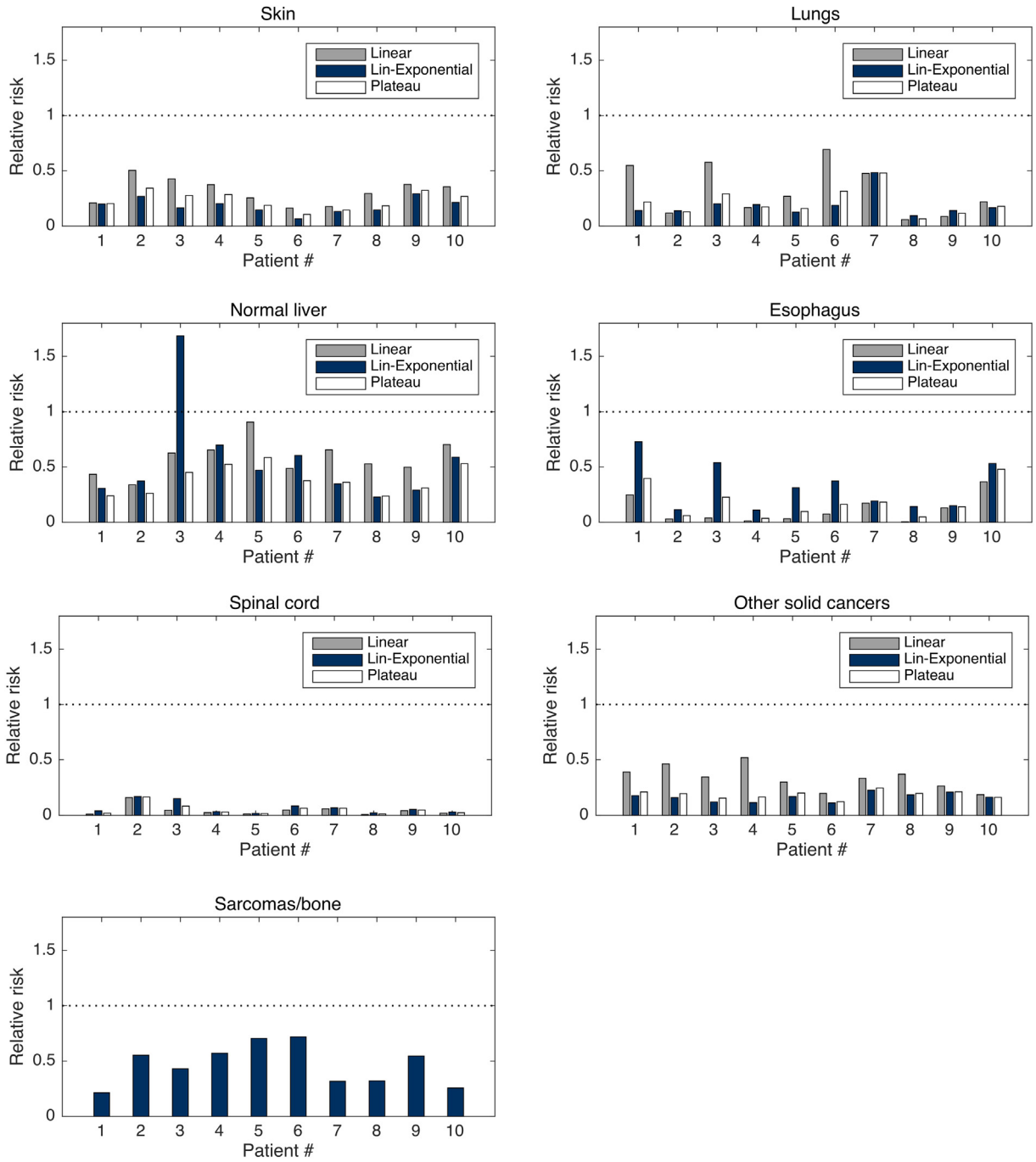

Fig. 3. The relative risks of observing carcinomas (skin, lungs, healthy part of the liver, esophagus, spinal cord and other solid tissue) and sarcomas (bone), estimated using the Schneider-model.

around the CTV leads to increased risks of secondary malignancies due to larger volumes of the surrounding healthy tissue included in the PTV [32]. The implementation of image-guided radiation therapy (IGRT) [33,34] in treatments involving moving targets will enable a reduction of the margins added around the CTV, and thereby a reduction of the doses given to the OARs. There is also a slight increase in the radiation-induced cancer-risk associated with imaging which should not be neglected [35,36].

It has been suggested that radiosurgery could reduce the frequency of secondary cancers, compared to conventional fractionation. In a study performed by Murray et al. [37], hypofractionated RT of prostate cancer reduced the risks of radiation-induced cancers compared to conventional fractionation schemes. This was found to be the case irrespective of the OAR location in relation to the treated volume. In a study performed by Dasu and coworkers [32], hypofractionation resulted in slightly increased risks for bladder- and rectal-cancer. The increased cancer-risk was observed in the organs located closer to the irradiated tumour volumes. On the other hand, due to a reduced fluence of out-of-field radiation, hypofractionation produced decreased cancer-risks in the volumes located farther away from the target.

In our study, the demonstrated advantage of PBS, in terms of cancer-risk reduction, is related to the reduced integral doses given to the patients, compared to the corresponding photon plans. To minimize the irradiation of the healthy tissues in the proton plans, it was found advantageous to use as few beams as possible.

Clinical data regarding the long-term cancer incidence after proton RT is limited. Published short-term follow-up studies can be used for prospective evaluation of the treatment outcome in terms of secondary-cancer induction. In a short-term follow-up study, Chung et al. [38] compared the cancer incidence in a cohort of 558 adult patients (median age 59 years) which received proton therapy with another 558 adult patients which received photon-beam RT. The proton beam treatments resulted in a lower frequency of secondary malignancies (5.2%) compared to the photon-beam treatments (7.5%). However, the secondary cancer incidence has, in a study performed by Brenner et al. [39], been shown to increase considerably with the follow-up time. In this long-term follow-up study, the cancer incidence in prostate-cancer patients, which received photon-beam RT, was compared to those prostate-cancer patients previously treated with surgery alone. A comparable level of the risk of secondary cancer was obtained for the bladder (15%) and lungs (11%), even though one of these patient-groups was not irradiated at all. Our results show a relative reduction in the organ-specific cancer risks with PBS, without necessarily providing the accurate absolute values of these cancer risks. The relative reduction of cancer-risk could be less important if the overall absolute risks are very low.

The patients included in this study were adult patients diagnosed with liver metastases late in life. Lower risks of secondary-cancer induction have been reported for elderly RT cancer patients [40], mostly due to the short life expectancy compared to the time required for the carcinogenesis process to take place. The results obtained for the patient group included in this study, can potentially serve as a guideline for ranking between the two RT modalities compared, taking into account the levels of cancer-induction which can be expected after completed RT.

The model parameters used in this work for the assessment of treatment-induced cancer risks were derived from epidemiological studies. Apart from the uncertainties in the epidemiological data [41], there are considerable uncertainties associated with the predictions of radiotherapy-induced cancers connected to other factors. For example, the inter-patient variation of the target size and location determines the irradiation configuration used for the photon- and proton-beam treatments. In this context, the use of ratios of risks in a pairwise comparison of different RT modalities may be useful for ranking RT modalities [41]. In this work, the risk of radiation induced-secondary cancers in different OARs after IMPT was studied using established model-parameters, obtained from the experience with photon-beam RT, assuming that the radiobiological effect of proton beams is similar to what it is for photon beams. The expected future increase in the clinical use of proton beams for cancer treatment will provide further information regarding the tissue response to proton-beam irradiation.

5. Conclusions

The results of this study indicate that, with IMPT-based radiosurgery of liver metastases, a reduction of the risks of radiation-induced secondary cancers can be achieved, compared to photon-beam based SBRT treatments. Despite the fact that the predicted cancer-risks were model-dependent, lower risks were obtained with IMPT, irrespective of the dose-response relationship used.

Funding

This study was financially supported by the Swedish International Development Cooperation Agency (SIDA) through the International Science Programme (ISP) and the Cancer Research Funds of *Radiumhemmet* at Karolinska Institute, Stockholm, Sweden.

Conflicts of interest

None.

Acknowledgements

The authors would like to acknowledge Maja Malmberg for the valuable comments and critical suggestions, which strongly contributed to this report.

References

[1] Miralbell R, Lomax A, Cella L, Schneider U. Potential reduction of the incidence of radiation-induced second cancers by using proton beams in the treatment of pediatric tumors. Int J Radiat Oncol 2002;54:824–9. http://dx.doi.org/10.1016/S0360-3016(02)02982-6.

[2] Yock TI, Caruso PA. Risk of second cancers after photon and proton radiotherapy: a review of the data. Health Phys 2012;103:577–85. http://dx.doi.org/10.1097/HP.0b013e3182609ba4.

[3] Yoon M, Ahn SH, Kim J, Shin DH, Park SY, Lee SB, et al. Radiation-induced cancers from modern radiotherapy techniques: intensity-modulated radiotherapy versus proton therapy. Int J Radiat Oncol Biol Phys 2010;77:1477–85. http://dx.doi.org/10.1016/j.ijrobp.2009.07.011.

[4] Paganetti H, Athar BS, Moteabbed M, Adams J, Schneider U, Yock T. Assessment of radiation-induced second cancer risks in proton therapy and IMRT for organs inside the primary radiation field. Phys Med Biol 2012;57:6047–61. http://dx.doi.org/10.1088/0031-9155/57/19/6047.

[5] Paganetti H, van Luijk P. Biological considerations when comparing proton therapy with photon therapy. Semin Radiat Oncol 2012. http://dx.doi.org/10.1016/j.semradonc.2012.11.002.

[6] Greco C, Wolden S. Current status of radiotherapy with proton and light ion beams. Cancer 2007;109:1227.

[7] Björk-Eriksson T, Glimelius B. The potential of proton beam therapy in paediatric cancer. Acta Oncol (Madr) 2005;44:871–5. http://dx.doi.org/10.1080/02841860500355959.

[8] Hardy P, Bridge P. What are the potential benefits and limitations of particle therapy in the treatment of paediatric malignancies? J Radiother Pract 2008;7:9–18. http://dx.doi.org/10.1017/S1460396907006218.

[9] de Gonzalez AB, Curtis RE, Kry SF, Gilbert E, Lamart S, Berg CD, et al. Proportion of second cancers attributable to radiotherapy treatment in adults: a cohort study in the US SEER cancer registries. Lancet Oncol 2011;12:353–60. http://dx.doi.org/10.1016/S1470-2045(11)70061-4.

[10] Vanderwalde AM, Hurria A. Second malignancies among elderly survivors of cancer. Oncologist 2011;16:1572–81. http://dx.doi.org/10.1634/theoncologist.2011-0214.

[11] Preston DL, Ron E, Tokuoka S, Funamoto S, Nishi N, Soda M, et al. Solid cancer incidence in atomic bomb survivors: 1958–1998. Radiat Res 2007;168:1–64.

[12] Stewart A. A-bomb data: detection of bias in the life span study cohort. Environ Health Perspect 1997;105:1519–21.

[13] Heidenreich WF, Cullings HM. Use of the individual data of the a-bomb survivors for biologically based cancer models. Radiat Environ Biophys 2010;49:39–46. http://dx.doi.org/10.1007/s00411-009-0253-9.

[14] Li CI, Nishi N, McDougall JA, Semmens EO, Sugiyama H, Soda M, et al. Relationship between radiation exposure and risk of second primary cancers among atomic bomb survivors. Cancer Res 2010;70:7187–98. http://dx.doi.org/10.1158/0008-5472.CAN-10-0276.

[15] Daşu A, Toma-Daşu I, Olofsson J, Karlsson M. The use of risk estimation models for the induction of secondary cancers following radiotherapy. Acta Oncol (Madr) 2005;44:339–47. http://dx.doi.org/10.1080/02841860510029833.

[16] Schneider U, Zwahlen D, Ross D, Kaser-Hotz B. Estimation of radiation-induced cancer from three-dimensional dose distributions: concept of organ equivalent dose. Int J Radiat Oncol Biol Phys 2005;61:1510–5. http://dx.doi.org/10.1016/j.ijrobp.2004.12.040.

[17] UNSCEAR. Sources and Effects of Ionizing Radiation 1993 Report to the General Assembly with Scientific Annexes. New York, 1993.

[18] Schneider U. Mechanistic model of radiation-induced cancer after fractionated radiotherapy using the linear-quadratic formula. Med Phys 2009;36:1138–43. http://dx.doi.org/10.1118/1.3089792.

[19] Schneider U, Besserer J, Hartmann M. Hypofractionated radiotherapy has the potential for second cancer reduction. Strahlentherapie Und Onkol 2013;189:1078.

[20] Liu E, Stenmark MH, Schipper MJ, Balter JM, Kessler ML, Caoili EM, et al. Stereotactic body radiation therapy for primary and metastatic liver tumors. Transl Oncol 2013;6:442–6.

[21] Lee MT, Kim JJ, Dinniwell R, Brierley J, Lockwood G, Wong R, et al. Phase I study of individualized stereotactic body radiotherapy of liver metastases. J Clin Oncol 2009;27:1585–91. http://dx.doi.org/10.1200/JCO.2008.20.0600.

[22] Fukumitsu N, Okumura T, Takizawa D, Makishima H, Numajiri H, Murofushi K, et al. Proton beam therapy for metastatic liver tumors. Radiother Oncol 2015;117:322–7. http://dx.doi.org/10.1016/j.radonc.2015.09.011.

[23] Petersen JBB, Lassen Y, Hansen AT, Muren LP, Grau C, Hyer M. Normal liver tissue sparing by intensity-modulated proton stereotactic body radiotherapy

for solitary liver tumours. Acta Oncol 2011;Vol 50(6):823–8. doi:10.3109/0284186X.2011.590526.
[24] Mondlane G, Gubanski M, Lind P, Henry T, Ureba A, Siegbahn A. Dosimetric comparison of plans for photon- or proton-beam based radiosurgery of liver metastases. Int J Part Ther 2016;3:277–84. http://dx.doi.org/10.14338/IJPT-16-00010.1.
[25] ICRP Publication 103. The 2007 Recommendations of the International Commission on Radiological Protection. 2007.
[26] Schneider U, Lomax A, Pemler P, Besserer J, Ross D, Lombriser N, et al. The impact of IMRT and proton radiotherapy on secondary cancer incidence. Strahlentherapie Und Onkol Organ Der Dtsch Rontgengesellschaft [et al.] 2006;182:647–52. http://dx.doi.org/10.1007/s00066-006-1534-8.
[27] Schneider U, Hälg R. The impact of neutrons in clinical proton therapy. Front Oncol 2015:5. doi:10.3389/fonc.2015.00235.
[28] Taddei PJ, Howell RM, Krishnan S, Scarboro SB, Mirkovic D, Newhauser WD. Risk of second malignant neoplasm following proton versus intensity-modulated photon radiotherapies for hepatocellular carcinoma. Phys Med Biol 2010;55:7055–65. http://dx.doi.org/10.1088/0031-9155/55/23/S07.
[29] Schneider U, Agosteo S, Pedroni E, Besserer J. Secondary neutron dose during proton therapy using spot scanning. Int J Radiat Oncol Biol Phys 2002;53:244–51. http://dx.doi.org/10.1016/S0360-3016(01)02826-7.
[30] Dawson LA, Ten Haken RK. Partial volume tolerance of the liver to radiation. Semin Radiat Oncol 2005;15:279–83. http://dx.doi.org/10.1016/j.semradonc.2005.04.005.
[31] Nair VJ, Pantarotto JR. Treatment of metastatic liver tumors using stereotactic ablative radiotherapy. World J Radiol 2014;6:18–25. http://dx.doi.org/10.4329/wjr.v6.i2.18.
[32] Daşu A, Toma-Daşu I, Franzén L, Widmark A, Nilsson P. Secondary malignancies from prostate cancer radiation treatment: a risk analysis of the influence of target margins and fractionation patterns. Int J Radiat Oncol 2011;79:738–46. http://dx.doi.org/10.1016/j.ijrobp.2009.12.004.
[33] Jaffray DA. Image-guided radiotherapy: from current concept to future perspectives. Nat Rev Clin Oncol 2012;9:688–99.
[34] Shimizu S, Miyamoto N, Matsuura T, Fujii Y, Umezawa M, Umegaki K. A proton beam therapy system dedicated to spot-scanning increases accuracy with moving tumors by real-time imaging and gating and reduces equipment size. (Report). PLoS One 2014:9.
[35] Ardenfors O, Josefsson D, Dasu A. Are IMRT treatments in the head and neck region increasing the risk of secondary cancers? Acta Oncol (Madr) 2014;53:1041–7. http://dx.doi.org/10.3109/0284186X.2014.925581.
[36] Hess CB, Thompson HM, Benedict SH, Seibert JA, Wong K, Vaughan AT, et al. Exposure risks among children undergoing radiation therapy: considerations in the era of image guided radiation therapy. Int J Radiat Oncol 2016;94:978–92. http://dx.doi.org/10.1016/j.ijrobp.2015.12.372.
[37] Murray LJ, Thompson CM, Lilley J, Cosgrove V, Franks K, Sebag-Montefiore D, et al. Radiation-induced second primary cancer risks from modern external beam radiotherapy for early prostate cancer: impact of stereotactic ablative radiotherapy (SABR), volumetric modulated arc therapy (VMAT) and flattening filter free (FFF) radiotherapy. Phys Med Biol 2015;60:1237–57. http://dx.doi.org/10.1088/0031-9155/60/3/1237.
[38] Chung CS, Yock TI, Nelson K, Xu Y, Keating NL, Tarbell NJ. Incidence of second malignancies among patients treated with proton versus photon radiation. Int J Radiat Oncol Biol Phys 2013;87:46–52. http://dx.doi.org/10.1016/j.ijrobp.2013.04.030.
[39] Brenner DJ, Curtis RE, Hall EJ, Ron E. Second malignancies in prostate carcinoma patients after radiotherapy compared with surgery. Cancer 2000;88:398–406. http://dx.doi.org/10.1002/(SICI)1097-0142(20000115)88:2<398::AID-CNCR22>3.0.CO.
[40] Fraumeni J, Curtis R, Edwards B, Tucker M. Introduction. In: Curtis R, Freedman D, Ron E, Ries L, Hacker D, Edwards B, editors. New Malig among cancer Surviv SEER cancer Regist 1973–2000. Bethseda, USA: National Cancer Institute Publ No 05-5302; 2006.
[41] Kry SF, Followill D, White RA, Stovall M, Kuban DA, Salehpour M. Uncertainty of calculated risk estimates for secondary malignancies after radiotherapy. Int J Radiat Oncol 2007;68:1265–71. http://dx.doi.org/10.1016/j.ijrobp.2007.04.014.
[42] Kehwar T. Analytical approach to estimate normal tissue complication probability using best fit of normal tissue tolerance doses into the NTCP equation of the linear quadratic model. J Cancer Res Ther 2005;1:168–79.